H-7 Effects on the Structure and Fluid Conductance of Monkey Trabecular Meshwork

Ilana Sabanay, PhD; B'Ann T. Gabelt, MS; Baohe Tian, MD; Paul L. Kaufman, MD; Benjamin Geiger, PhD

Objective: To determine the effects of H-7 (1-[5-isoquinoline sulfonyl]-2-methyl piperazine) on the structure and fluid conductance of the trabecular meshwork of live cynomolgus monkeys.

Methods: Fluid outflow was measured by constant pressure perfusion of the anterior chamber with cationized and noncationized gold solution with or without H-7 in opposite eyes. The eyes were fixed by infusing Ito solution and enucleated. Anterior segments were cut into 4 sections, fixed in immersion solution, and embedded in epoxy resin-812. Trabecular meshwork morphologic features were studied by light and electron microscopy.

Results: H-7 affected trabecular meshwork organization and increased fluid outflow. H-7 expanded the intercellular spaces in the juxtacanalicular meshwork, accompanied by removal of extracellular material. The inner wall cells of the Schlemm canal became highly extended, yet cell-cell junctions were maintained. Colloidal gold particles were detected only in limited areas along the subcanalicular region in control eyes; after H-7 treatment, gold was widely seen along the entire inner canal wall. Most inner wall cells in H-7–treated eyes, but only few cells in control eyes, contained gold-loaded vesicles.

Conclusion: H-7 inhibits cell contractility, leading to "relaxation" of the trabecular outflow pathway, expanding the draining surface, and permitting more extensive flow through the meshwork.

Clinical Relevance: By inhibiting cellular contractility and relaxing the trabecular meshwork, the protein kinase inhibitor H-7 increases outflow facility and reduces intraocular pressure and thus has potential as an ocular hypotensive antiglaucoma medication.

Arch Ophthalmol. 2000;118:955-962

From the Department of Molecular Cell Biology, Weizmann Institute of Science, Rehovot, Israel (Drs Sabanay and Geiger); and the Department of Ophthalmology and Visual Sciences, University of Wisconsin, Madison (Ms Gabelt and Drs Tian and Kaufman).
The University of Wisconsin, Madison, and the Weizmann Institute of Science hold a patent related to this article; accordingly, Drs Kaufman and Geiger have a proprietary interest in the article. Alcon Laboratories, Inc, Fort Worth, Tex, has paid a fee to Drs Kaufman and Geiger for an option to license this technology and has provided some financial support in this general area. Dr Kaufman has also served as a paid consultant on unrelated issues for Alcon Laboratories, Inc, and several other pharmaceutical corporations.

IN PRIMATE AND human eyes, most aqueous humor outflow occurs via the trabecular meshwork (TM) and the Schlemm canal (SC).[1,2(pp251-280,307-335)] The TM consists of arrays of collagen beams covered by endothelial-like cells. The intertrabecular spaces through which the fluid flows are quite large at the innermost uveal TM and become narrower at the outer corneoscleral aspect.[3] The juxtacanalicular (JXT) region of the TM, close to the inner wall (IW) of the SC, has no collagenous beams but rather contains several layers of cells in contact with one another, immersed in loose extracellular material (ECM). The IW cells of the SC form a continuous lining and contain multiple vesicles, including giant vacuoles that are the hallmark of these cells.[2(pp89-123),4]

Glaucoma is characterized by progressive optic neuropathy usually associated with an elevated intraocular pressure (IOP), in turn consequent to abnormally high flow resistance in the TM.[2(pp89-123)] Despite extensive studies,[2(pp89-123),5] the exact location of the major outflow resistance barrier along the TM-SC pathway is still not clear in either the normal or the glaucomatous eye. Based on anatomical and physiological considerations, the cells and/or ECM in the JXT region or the IW cells of the SC are candidates.[6-9]

The cytoskeleton and, in particular, the actin-containing microfilament system help maintain cell shape and adhesive interactions. Researchers[10] have examined various microfilament reagents for their effect on outflow resistance.[11-17] The serine-threonine kinase inhibitor H-7 (1-[5-isoquinoline sulfonyl]-2-methyl piperazine) can perturb the actin cytoskeleton in cultured cells[17,18] and decrease outflow resistance in the TM in live monkey eyes and enucleated porcine eyes.[13,14,17] H-7 blocks actomyosin-driven contractility,[18-20] yet the mechanism of its effect on the aqueous outflow pathway in vivo remains unclear.

To elucidate this mechanism, we perfused the anterior chamber (AC) of op-

MATERIALS AND METHODS

ANIMALS AND ANESTHESIA

Three normal male cynomolgus monkeys (*Macaca fascicularis*), weighing 4 to 6 kg, were studied in accordance with University of Wisconsin, Madison, and National Institutes of Health, Bethesda, Md, guidelines. Anesthesia was intramuscular ketamine hydrochloride, 10 mg/kg, followed by intramuscular pentobarbital sodium, 35 mg/kg.

CHEMICALS AND DRUG PREPARATION

H-7 was obtained from Sigma-Aldrich Corp, St Louis, Mo. Cationic colloidal gold (5-nm particles; 5×10^{13} particles per milliliter in 20% glycerol) and bovine serum albumin–conjugated gold (10-nm particles; 5.7×10^{12} particles per milliliter in 20% glycerol and 1% bovine serum albumin; optical density=3.13 at 520 nm) were obtained from British BioCell International, Ltd, Cardiff, United Kingdom, distributed by Gold Mark Biologicals, Phillipsburg, NJ. Bovine serum albumin–conjugated gold (≈4 mL) was dialyzed before use against Bárány solution.[21] The optical density of the final solution was 1.7; 3.88 mL of solution had the same number of particles as 240 µL of cationized gold. Vehicle plus gold solution was formulated as follows: 7.88 mL of Bárány solution+240 µL of cationized gold (5-nm particles)+3.88 mL of dialyzed noncationized gold albumin (10-nm particles), so that the final solution contained equal concentrations (1×10^{12} particles per milliliter) of 5-nm cationized gold particles and 10-nm particles of noncationized gold conjugated to albumin. H-7, 300 µmol/L, was formulated as follows: 6 mL of vehicle plus gold solution+0.655 mg of H-7.

FLUID OUTFLOW MEASUREMENTS

Previous studies[13,14] have shown that H-7 significantly increases total and trabecular outflow facility in living monkeys. Therefore, we did not believe it was necessary to replicate those findings by the long-duration (minimum, 30-45 minutes) perfusion at 2 different pressures after drug administration required to obtain reliable postdrug facility measurement. Rather, we designed our protocol to do the following: (1) assure that the conventional outflow pathways of the 2 eyes of each individual animal were functionally normal and reasonably similar at the start, (2) minimize the possibility of perfusion-induced artifacts confounding drug-induced changes in TM morphologic features by shortening the postdrug perfusion duration, (3) still maintain a reasonable flow rate through the TM to assure adequate exposure of the entire pathway to a uniform drug concentration for a long enough duration for a drug effect to occur, and (4) obtain at least some physiological evidence of drug effect before humanely sacrificing a monkey for the structural studies. The shortened single-pressure postdrug perfusion precluded calculation of outflow facility but had the additional benefit of reducing the amount of expensive gold tracer.

Baseline (BL) outflow and outflow facility were determined by 2-level constant pressure perfusion of the AC with Bárány solution from an external reservoir,[21,22] alternating pressures of 25 and 35 mm Hg. Postdrug or postvehicle outflow was measured by constant pressure perfusion only at 25 mm Hg. All monkeys had undergone prior perfusions but not within the preceding 5 to 6 weeks; all posite eyes of live cynomolgus monkeys with fluid containing a flow tracer consisting of a mixture of cationized and noncationized colloidal gold with or without H-7, after which the morphologic features of the TM and SC were studied by light and electron microscopy.

RESULTS

FLUID OUTFLOW

For the 3 animals, the outflow ratios ([H-7 Rx/H-7 BL]/[vehicle Rx/vehicle BL]) were 2.18, 2.15, and 1.49. Analysis of these ratios on a log scale yields an estimated ratio of 1.91, indicating an H-7–induced outflow rate increase of 91% (95% confidence interval, 11%-230%; $P=.04$). As shown in **Figure 1** for the "demonstration" animal, the rate of fluid flow from the reservoir into the H-7–treated eye approximately doubled relative to BL and to the contralateral eye. Differences between BL mean outflow rates in the 2 eyes were not significant (BL of H-7 – BL of vehicle = 1.10 ± 0.62 µL/min, $P>.05$). The postdrug outflow rate, corrected for BL, in the H-7–treated eye significantly exceeded that in the vehicle-treated eye ([H-7 – BL] – [vehicle – BL] = 5.95 ± 0.89 µL/min, $P<.001$). In all 3 control eyes, the postvehicle outflow rate was less than the BL rate, but the average difference (–3.35 ± 1.43 µL/min) was not significant because of the large variability ($P=.14$; 95% confidence interval, –2.80 to 9.49). The decrease in outflow in the control eye was significant in the demonstration animal (vehicle Rx – vehicle BL = –2.07 ± 0.63 µL/min, $P=.001$).

MORPHOLOGIC FEATURES OF THE TM AND SC

Light microscopy revealed distention of the JXT and SC areas after H-7 treatment (**Figure 2**, A and B), with little or no effect on the uveal and corneoscleral regions of the TM. Low-power electron microscopy showed substantially increased intercellular spaces and almost complete loss of electron-dense ECM from the JXT region (Figure 2, C and D, and **Figure 3**, A and B), accompanied by a dramatic reduction in intercellular contacts between JXT cells. The effect of H-7 on the uveal meshwork was limited to mild retraction of the TM cells from their collagen beams, without apparent loss of cells (Figure 2, E and F).

Examination at a higher power (Figure 3, A and B) revealed that in the absence of H-7, gold particles (cationized and noncationized) were restricted to only limited JXT and subcanalicular areas. Typically, gold particles were detected in sparse foci corresponding to only 10% to 20% of the canal length (Figure 3, A), with spo-

were free of AC cells and flare by slitlamp biomicroscopy. The AC of both eyes was cannulated with a branched needle connected to a reservoir and pressure transducer and an unbranched needle with tubing clamped off. Following 35-minute BL outflow measurement, the clamped tubing from the unbranched needle was connected to syringes containing vehicle plus gold solution with or without H-7, 300 µmol/L, in contralateral eyes. The syringes were placed in a variable-speed infusion pump, and the tubing to the reservoir was opened to air, allowing infusion of 2 mL of vehicle plus gold solution with or without H-7, 300 µmol/L, through the AC for approximately 12 minutes (≈0.17 mL/min), maintaining an IOP at approximately 10 to 15 mm Hg. The reservoirs were emptied, filled with the identical solution as perfused through the eye, and reconnected to the eye, and the syringe tubing was clamped. The reservoirs were closed for the next 30 minutes without external fluid flowing into the eyes, and then reopened so that vehicle plus gold with or without H-7 solution flowed into each eye for 15 minutes, during which the IOP was maintained at 25 mm Hg.

For data analysis, the linear regression of cumulative volume on time for each monkey at each perfusion segment (H-7 BL, H-7 postexchange [Rx], vehicle BL, and vehicle Rx) was obtained. The ratio of these slopes ([H-7 Rx/H-7 BL]/[vehicle Rx/vehicle BL]) was calculated for each animal. Because the variability of the ratios on a log scale is probably more normal, a 2-tailed paired *t* test was done on the logarithm of these ratios. For illustrative purposes, the data were further analyzed for the monkey with the most balanced BLs between eyes, as follows: the mean±SEM outflow rates were based on observed rates for 5- and 10-second intervals. The BL measurements contained 3 ten-second and 185 five-second intervals. The Rx measurements contained 178 five-second intervals. For each interval, the observed outflow rate was computed as follows: (cumulative volume at end of interval – cumulative volume at beginning of interval)/length of interval. An analysis of variance was used to compare the mean outflow rates for the perfusion segments (H-7 BL, H-7 Rx, vehicle BL, and vehicle Rx) with SEs based on a pooled variance estimate. *t* Tests were used to compare differences between mean outflow rates. Statistical software (SAS Proc Mixed) was used for the analyses.[23] For all the analyses, BL flow values for the 4 periods at 25 mm Hg were used, since the Rx measurements were all obtained at that pressure.

LIGHT AND ELECTRON MICROSCOPY OF THE TM

The inflow tubing was switched to reservoirs containing Ito fixative,[24] which was allowed to flow into the eyes for 40 to 90 minutes at 25 mm Hg. Both eyes were then enucleated under supplemental pentobarbital anesthesia just before euthanatizing by pentobarbital overdose. The anterior segment was cut into 4 sections, placed in Ito fixative, and embedded in epoxy resin-812 (SPI-PON; SPI, West Chester, Pa). Specimens for light microscopy were sectioned (2 µm) with an ultramicrotome (Ultracut E; Reichert-Jung, Vienna, Austria), stained with epoxy tissue (EMS, Fort Washington, Pa), and examined with a microscope (Zeiss Axiophot; Zeiss, Oberkochen, Germany). All 4 quadrants in all eyes were checked by light microscopy. Only regions that were grossly intact were examined by electron microscopy, usually 2 to 3 quadrants per specimen. For transmission electron microscopy, 700 Å sections were cut in the ultramicrotome, stained with uranyl acetate and lead citrate, and examined with a transmission electron microscope (model EM410 or CM12; Philips, Eindhoven, Holland).

radic scatterings of individual gold particles occasionally seen in other areas. Following H-7 treatment, the gold tracer was distributed much more broadly and uniformly. This diffuse distribution after H-7 treatment was consistent, with no apparent differences between different quadrants. The local densities were variable but typically were several-fold higher than in control eyes and were detected along most (usually >80%) of the canal length (Figure 3, B). In control and H-7–treated eyes, we occasionally noticed highly dense local gold deposits; such areas were discarded. The gold particles in control eyes were associated with ECM throughout the JXT region, while in the H-7–treated eyes they were mainly associated with the residual matrix in proximity to the IW cells (Figure 3, B). A representative 183-µm segment of the JXT space of a control eye revealed 380 gold particles located in several distinct foci (Figure 3, C). In an H-7–treated eye, the density of gold particles was nearly 5-fold higher (2427 particles per 239 µm) and the gold was widely distributed throughout the JXT region (Figure 3, D).

In H-7–treated eyes, more IW cells contained giant vacuoles and the vacuoles were larger, compared with controls (**Figure 4**, A and B). Untreated IW cells varied in basal-to-lumenal thickness and usually contained arrays of densely packed intermediate filaments (Figure 4, C). Following H-7 treatment, the tight organization of the cytoskeleton was apparently perturbed (Figure 4, D) and the cells generally adopted a flatter, wider, "relaxed" appearance. The mean±SD cell junction-to-junction distance was 3.3±2.0 µm in control eyes vs 5.6±3.0 µm after H-7 treatment (Figure 3, C and D) (values based on measurement of 62 and 109 cells in 3 pairs of H-7–treated and vehicle-treated eyes, respectively), suggesting that the basal area of the cells was at least tripled. However, the continuity of the canal wall was well preserved, and the junctions between neighboring cells were not affected (Figure 4, C and D). Careful examination of the interface between IW cells indicated that gold particles reached the basal aspects of intercellular junctions but never crossed them toward the lumen of the SC (Figure 4, G).

The main route through which gold particles were transported from the basal aspect of the IW into the canal lumen was via numerous vesicles, ranging from approximately 60 to 350 nm (Figure 4, E and F). Some vesicles contained only few gold particles, while others were loaded with gold. H-7 treatment markedly increased the percentage of cells containing gold-loaded vesicles and the number of gold particles per vesicle. The intravesicular gold was associated with electron-dense material similar to the ECM found in the JXT region in untreated eyes.

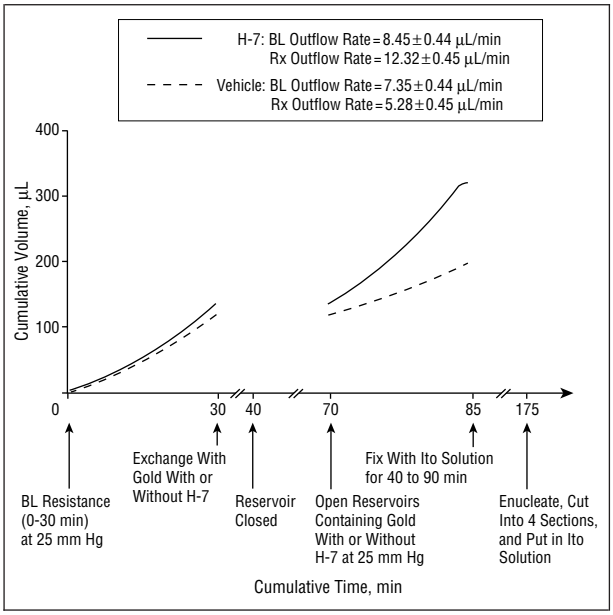

Figure 1. *Mean ± SEM effect of anterior chamber exchange with H-7 (1-[5-isoquinoline sulfonyl]-2-methyl piperazine), 300 µmol/L, on outflow in a cynomolgus monkey. Contralateral baseline (BL) outflow rates are not significantly different. The postdrug outflow rate, corrected for BL, in the H-7–treated eye is greater than that in the vehicle-treated eye by 5.95 ± 0.89 µL/min (P<.001). The postvehicle outflow rate is less than the BL in the vehicle-treated eye by 2.07 ± 0.63 µL/min (P<.001). Rx indicates postexchange.*

COMMENT

Intracameral or topical application of H-7 to the living monkey eye reduces IOP by reducing flow resistance through the TM by up to 60%,[13,14] consistent with the flow rate measurements. H-7 induces apparent "relaxation" of JXT and IW cells, accompanied by an increase in JXT extracellular spaces, loss of JXT ECM, and establishment of new fluid flow pathways accessible to the gold particles used herein as flow tracers. However, despite this overall distention of the canalicular and JXT regions, tissue architecture and integrity are grossly maintained; in contrast, the actin-disrupting compounds cytochalasins B and D induce IW breaks.[10,16] The effect of H-7 on flow resistance is also reversible within 2 hours following drug removal[13] and, therefore, not attributable to irreversible toxicity. The postvehicle outflow rate in the control eyes tended to be reduced compared with BL, which differs from the typical finding in perfused monkey eyes that outflow facility increases over time, perhaps due to "washout" of resistance-relevant ECM.[25-27] The decrease could have been induced by gold particles, albumin, or both in the vehicle solution. We have previously shown that serum dose dependently decreases outflow facility in monkeys.[28]

H-7 is a broad-spectrum inhibitor of serine-threonine phosphorylation, affecting various kinases, including protein kinase C, myosin light chain kinase, and ρ kinase.[18,29-31] The present study and previous studies[18-20] suggest that the major relevant effect of H-7 is blocking cellular actomyosin-driven contractility, via inhibition of myosin light chain kinase, ρ kinase, or both.[30-32] Such a decrease in contractility is followed by a rapid deterioration of actin-containing stress fibers and focal contacts.[18,31]

Reduced flow resistance in pilocarpine-treated monkey eyes correlates best with the formation of apparently empty spaces in the sub-IW region.[33] Pilocarpine reduces flow resistance by contracting the ciliary muscle, which by virtue of the muscle's attachments to the TM, JXT region, and SC in turn "spreads" or "expands" these tissues.[34] Our data suggest that under normal conditions, the IW and JXT cells are in a contracted state and that reduction in their contractility can also expand these tissues and alter the routes and extent of fluid flow. Thus, in untreated eyes, flow (indicated by the presence of gold particles) is limited by reaching only part of the SC. The nature of the flow barriers that restrict or channel flow in the untreated eye is not clear,[35] but the apparent relaxation induced by H-7 enables fluid to flow through the entire TM, thus reaching the entire basal surface of the SC.

The corneoscleral and JXT areas of the TM in the nontreated eye contain large amounts of amorphous, electron-dense ECM,[26,36-41] thought to consist mainly of glycosaminoglycans.[42-44] It has been suggested that accumulation of this material in glaucomatous eyes may be responsible, at least in part, for the increased flow resistance.[39,45] There is evidence for the reciprocal mechanism, namely, that the accumulation of ECM occurs in the presence of a low rate of flow.[46] While the interrelations between flow resistance and accumulation of ECM are still unclear, and while we did not directly address this issue, the present results, showing numerous vesicles containing ECM associated with AC-infused tracer gold inside the IW cells in H-7–treated eyes, support the view that clearance of ECM from the JXT region involves active basal-to-lumenal transport by IW cells and that the primary effect of H-7 probably is an extension of the outflow pathways, rather than a direct effect on the ECM. H-7, administered topically or into the AC, may inhibit the contractility of cells in the distal region of the flow pathway, mainly in the JXT region and IW. The relaxation of these cells greatly expands the volume accessible to flow, thus resulting in lower resistance or higher facility. In the course of this process, most of the ECM normally deposited in the JXT region of untreated eyes is removed from that region. While we cannot exclude the possibility that washout of these ECM deposits is responsible, in part, for the decline in resistance, this does not appear to be the primary mechanism for H-7's effect. This reasoning is based on the previous observation[13] that the H-7–induced facility increase was reversed after a 2-hour waiting period with the external reservoir closed. Since presumably many hours would be required for resynthesis and deposition of ECM, the rapid reversibility seems to suggest the following: (1) that the observed loss of ECM may not be responsible for the H-7–induced outflow facility increase and/or (2) that redeposition of the lost ECM may not be involved in the reversibility mechanism. This could further suggest that ECM removal is probably a secondary, rather than a primary, event and even that the ECM may not be relevant to resistance at all. Morphologic studies of such "recovered" eyes would help answer this question, and are pending.

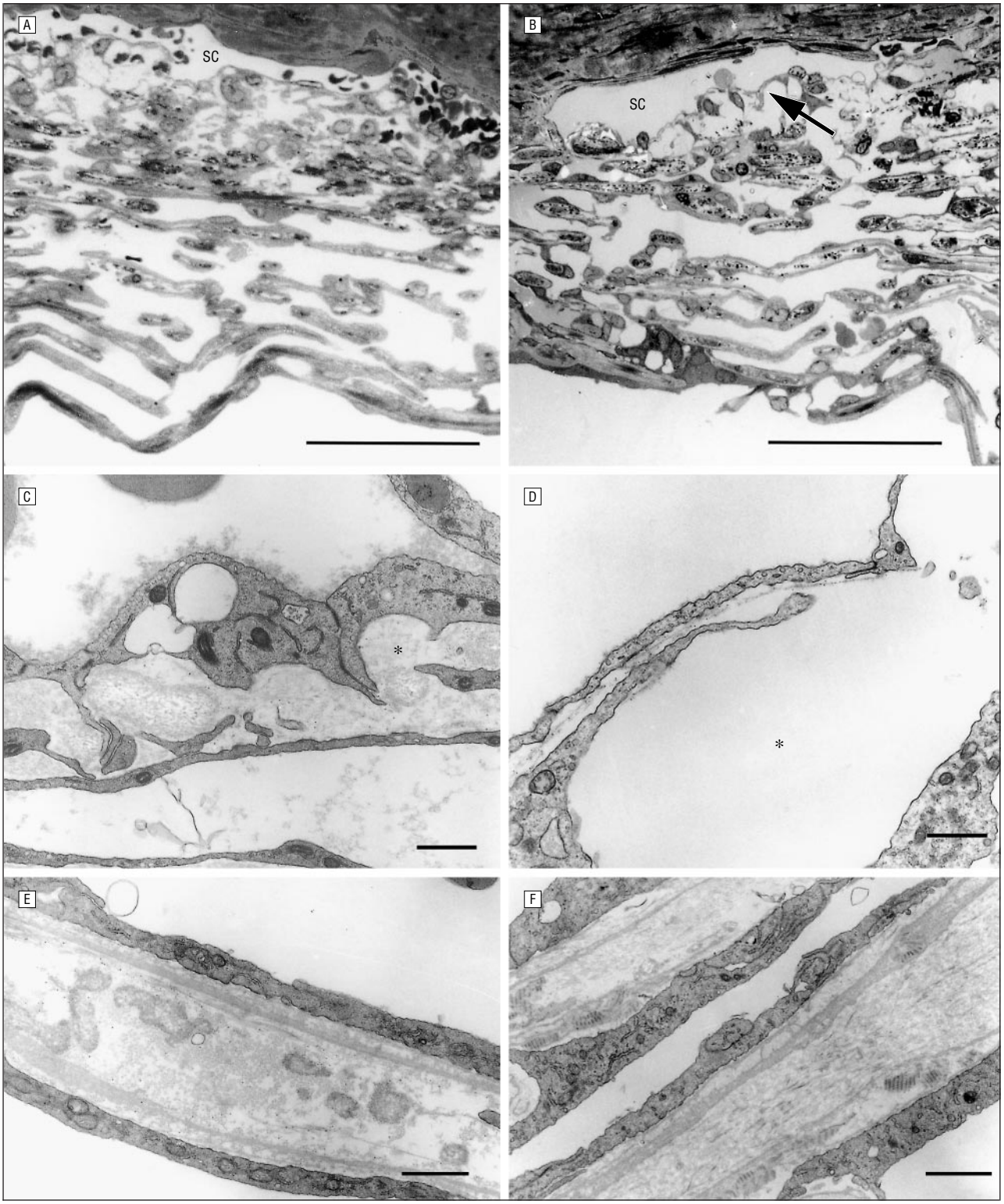

Figure 2. *Light micrographs (A-B; bars indicate 50 µm) and transmission electron micrographs (C-F; bars indicate 1 µm) of trabecular meshwork (TM) and Schlemm canal (SC) in monkey eyes treated with H-7 (1-[5-isoquinoline sulfonyl]-2-methyl piperazine), 300 µmol/L (B, D, and F), or vehicle (A, C, and E). The juxtacanalicular area (arrow in B) and intercellular spaces are extended, and extracellular material is lost (asterisks in C and D). Inner wall endothelial cells in H-7–treated eyes were thinner than in controls. Inner uveal TM (B) and trabecular cells associated with beams (E and F) were not significantly affected.*

One might also reasonably hypothesize that different deformations of the relaxed TM structure at a higher vs lower pressure or flow rate may be the mechanism for H-7's pressure- or flow-dependent facility increase, quick reversibility on cessation of perfusion, and progressive facility reincrease shortly after restarting perfusion even without drug.[13] At higher pressure or flow, the relaxed tissue could be extended or expanded further than at lower pressure or flow, where the relaxed tissue could be relatively retracted or folded. When the reservoir is closed,

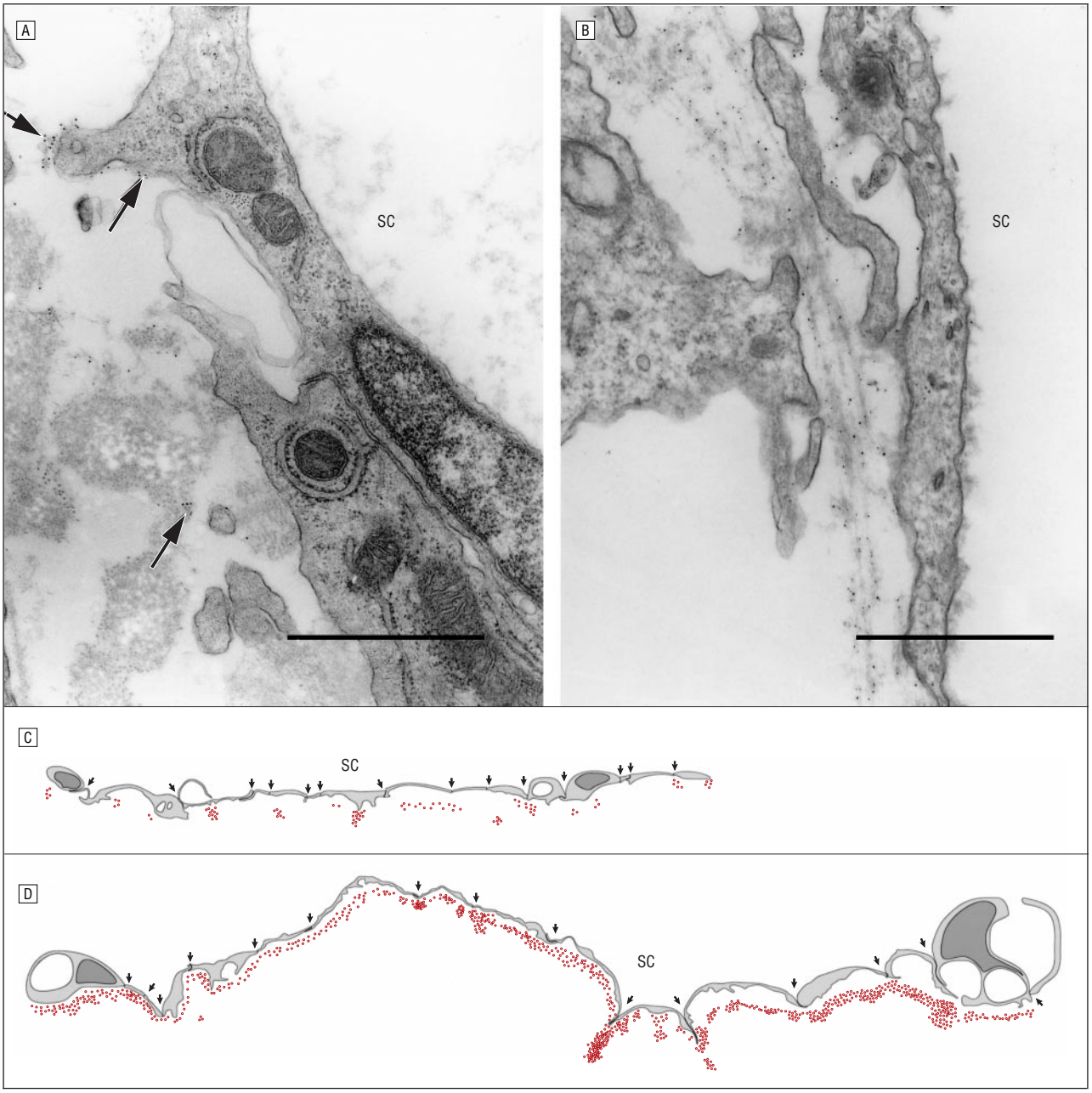

Figure 3. *Distribution of perfused gold particles in the juxtacanalicular area of eyes treated with H-7 (1-[5-isoquinoline sulfonyl]-2-methyl piperazine) and control eyes. A and B, Electron micrographs showing gold particle distribution under inner wall endothelial cells. There is focal distribution of gold particles in control eyes (arrows in A) compared with wide distribution following H-7 treatment (B). Bars indicate 1 µm. C and D, Schematic drawings depicting 15-cell stretches (cell-cell junctions marked by arrows) along the Schlemm canal (SC) of control (C) and H-7–treated (D) eyes. The location of individual gold particles is represented by red dots. Bars indicate 4 µm.*

spontaneous IOP is usually approximately 7 mm Hg in monkeys under pentobarbital anesthesia,[47] so that the pressure gradient between the AC and SC during the waiting period is either absent or much lower than under normal awake physiological conditions. Using this scenario, H-7 may be more effective in patients with glaucoma who have an elevated IOP, especially if they are not receiving secretory suppressants, while its effect may be less pronounced at a low IOP.

H-7 apparently does not interfere with (and perhaps even enhances) transcytosis of fluid and ECM across the IW cells into the lumen of the SC. H-7 induces an increase in pinocytic activity in neutrophils,[48] in line with the notion that endocytosis does not depend on H-7–sensitive myosin II activity. The data support that H-7 induces cellular relaxation, leading to increased levels of transcytosis or endocytosis of the gold tracer, which could be a mechanism contributing to the H-7–induced facility increase. However, it remains to be determined whether the facility increase is attributable to enhancement of the rate of endocytosis or to the wider distribution of the tracer in the JXT region. Our data do not support enhancement of fluid passage between IW cells.

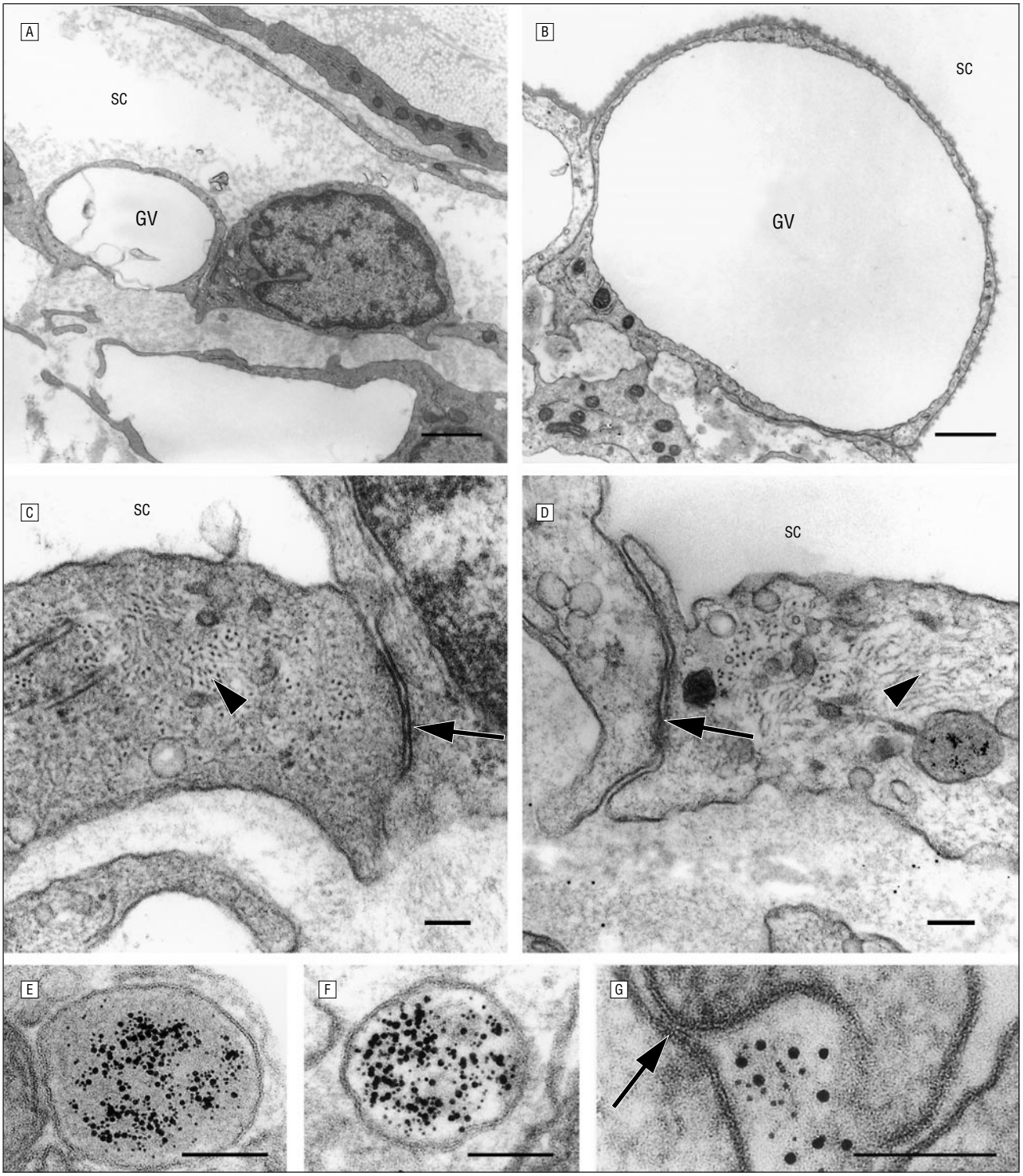

Figure 4. *Transmission electron micrographs of the effect of H-7 (1-[5-isoquinoline sulfonyl]-2-methyl piperazine) on inner wall (IW) cells of the Schlemm canal (SC). Control eyes are shown in A, C, and E; H-7–treated eyes, B, D, F, and G. Bars in A and B indicate 1 µm; in C through G, 0.1 µm. There is increased size of giant vacuoles (GVs) following H-7 treatment (A vs B). Dense arrays of cytoskeletal filaments (mostly intermediate filaments) (arrowheads in C and D) become loose after H-7 treatment; cell-cell junctions are unaffected (arrows in C and D). Gold particles (cationized and noncationized) are in numerous vesicles throughout IW cells (E and F). Extracellular subcanalicular gold reaches cell-cell junctions (arrow in G) but apparently does not penetrate through them.*

After many years of study, we still do not know the exact site or source of resistance to fluid drainage from normal or glaucomatous eyes. The present findings suggest that exclusion of large segments of the trabecular outflow pathway may help maintain high resistance to flow. Expanding the areas available for fluid drainage, by relaxation of the IW cells and the adjacent JXT region, either physiologically or pharmacologically (using compounds such as H-7), may be a possible approach to glaucoma therapy.

Accepted for publication December 8, 1999.

This study was supported by grants EY02698 and EY07119 from the National Eye Institute, Bethesda, Md; the American Health Assistance Foundation, Rockville, Md; the Glaucoma Research Foundation, San Francisco, Calif; Research to Prevent Blindness Inc, New York, NY; the Wisconsin Alumni Research Foundation, Madison; and the Ocular Physiology Research and Education Foundation, Madison. Dr Geiger is the incumbent of the E. Neter Chair in Cell and Tumor Biology at Weizmann Institute of Science, Rehovot, Israel.

We thank Alexander Bershadsky, PhD, for providing insightful discussions; Nili Sabanay for assisting with the quantitative analysis of gold particle distribution; and Lyndia Brumback, MS, and Ronald Gangnon, PhD, for statistically analyzing the flow data.

Reprints: Paul L. Kaufman, MD, Department of Ophthalmology and Visual Sciences, University of Wisconsin Clinical Science Center, 600 Highland Ave, Madison, WI 53792-3220 (e-mail: kaufmanp@mhub.ophth.wisc.edu).

REFERENCES

1. Millar JC, Gabelt BT, Kaufman PL. Aqueous humor dynamics. In: Tasman W, Jaeger EA, eds. *Duane's Clinical Ophthalmology.* Vol 3. Philadelphia, Pa: Lippincott-Raven Publishers; 1998:1-34.
2. Ritch R, Shields MB, Krupin T, eds. *The Glaucomas: Basic Sciences.* 2nd ed. St Louis, Mo: Mosby–Year Book Inc; 1996.
3. Ujiie K, Bill A. The drainage routes for aqueous humor in monkeys as revealed by scanning electron microscopy of corrosion casts. *Scanning Electron Micros.* 1984;1984(pt 2):849-856.
4. Epstein DL, Rohen JW. Morphology of the trabecular meshwork and inner-wall endothelium after cationized ferritin perfusion in the monkey eye. *Invest Ophthalmol Vis Sci.* 1991;32:160-171.
5. Buller C, Johnson D. Segmental variability of the trabecular meshwork in normal and glaucomatous eyes. *Invest Ophthalmol Vis Sci.* 1994;35:3841-3851.
6. Bill A, Svedbergh B. Scanning electron microscopic studies of the trabecular meshwork and the canal of Schlemm: an attempt to localize the main resistance to outflow of aqueous humor in man. *Acta Ophthalmol (Copenh).* 1972; 50:295-320.
7. Ethier CR, Kamm RD, Palaszewski BA, Johnson MC, Richardson TM. Calculations of flow resistance in the juxtacanalicular meshwork. *Invest Ophthalmol Vis Sci.* 1986;27:1741-1750.
8. Allingham RR, de Kater AW, Ethier CR, Anderson PJ. The relationship between pore density and outflow facility in human eyes. *Invest Ophthalmol Vis Sci.* 1992; 33:1661-1669.
9. Murphy CG, Johnson MC, Alvarado JA. Juxtacanalicular tissue in pigmentary and primary open angle glaucoma: the hydrodynamic role of pigment and other constituents. *Arch Ophthalmol.* 1992;110:1779-1785.
10. Johnson DH. The effect of cytochalasin D on outflow facility and the trabecular meshwork of the human eye in perfusion organ culture. *Invest Ophthalmol Vis Sci.* 1997;38:2790-2799.
11. Kaufman PL, Bárány EH. Cytochalasin B reversibly increases outflow facility in the eye of the cynomolgus monkey. *Invest Ophthalmol Vis Sci.* 1977;16:47-53.
12. Peterson JA, Tian B, Bershadsky AD, et al. Latrunculin-A increases outflow facility in the monkey. *Invest Ophthalmol Vis Sci.* 1999;40:931-941.
13. Tian B, Kaufman PL, Volberg T, Gabelt BT, Geiger B. H-7 disrupts the actin cytoskeleton and increases outflow facility. *Arch Ophthalmol.* 1998;116:633-643.
14. Tian B, Gabelt BT, Peterson JA, Kiland JA, Kaufman PL. H-7 increases trabecular facility and facility after ciliary muscle disinsertion in monkeys. *Invest Ophthalmol Vis Sci.* 1999;40:239-242.
15. Tian B, Gabelt BT, Kaufman PL. Effect of staurosporine on outflow facility in monkeys. *Invest Ophthalmol Vis Sci.* 1999;40:1009-1011.
16. Svedbergh B, Lütjen-Drecoll E, Ober M, Kaufman PL. Cytochalasin B–induced structural changes in the anterior ocular segment of the cynomolgus monkey. *Invest Ophthalmol Vis Sci.* 1978;17:718-734.
17. Epstein DL, Rowlette LL, Roberts BC. Acto-myosin drug effects and aqueous outflow function. *Invest Ophthalmol Vis Sci.* 1999;40:74-81.
18. Volberg T, Geiger B, Citi S, Bershadsky AD. Effect of protein kinase inhibitor H-7 on the contractility, integrity, and membrane anchorage of the microfilament system. *Cell Motil Cytoskeleton.* 1994;29:321-338.
19. Gills JP, Roberts BC, Epstein DL. Microtubule disruption leads to cellular contraction in human trabecular meshwork cells. *Invest Ophthalmol Vis Sci.* 1998; 39:653-658.
20. Tian B, Millar C, Kaufman PL, Bershadsky A, Becker E, Geiger B. H-7 effects on the iris and ciliary muscle in monkeys. *Arch Ophthalmol.* 1998;116:1070-1077.
21. Bárány EH. Simultaneous measurement of changing intraocular pressure and outflow facility in the vervet monkey by constant pressure infusion. *Invest Ophthalmol.* 1964;3:135-143.
22. Bárány EH. Relative importance of autonomic nervous tone and structure as determinants of outflow resistance in normal monkey eyes (*Cercopithecus ethiops* and *Macaca irus*). In: Rohen JW, ed. *The Structure of the Eye: Second Symposium.* Stuttgart, Germany: FK Schattauer Verlag; 1965:223-236.
23. Littel RC, Milliken GA, Stroup WW, Wolfinger RD. *SAS System for Mixed Models.* Cary, NC: SAS Institute Inc; 1996.
24. Ito S, Karnovsky MJ. Formadehyde-glutaraldehyde fixatives containing trinitro compounds [abstract]. *J Cell Biol.* 1968;39(suppl):168A-169A.
25. Erickson KA, Kaufman PL. Comparative effects of three ocular perfusates on outflow facility in the cynomolgus monkey. *Curr Eye Res.* 1981;1:211-216.
26. Knepper PA, Farbman AI, Telser AG. Exogenous hyaluronidases and degradation of hyaluronic acid in the rabbit eye. *Invest Ophthalmol Vis Sci.* 1984;25: 286-293.
27. Bárány EH, Woodin AM. Hyaluronic acid and hyaluronidase in the aqueous humor and the angle of the anterior chamber. *Acta Physiol Scand.* 1955;33: 257-290.
28. Kee C, Gabelt BT, Gange SJ, Kaufman PL. Serum effects on aqueous outflow during anterior chamber perfusion in monkeys. *Invest Ophthalmol Vis Sci.* 1996; 37:1840-1848.
29. Hidaka H, Inagaki M, Kawamoto S, Sasaki Y. Isoquinolinesulfonamides, novel and potent inhibitors of cyclic nucleotide dependent protein kinase and protein kinase C. *Biochemistry.* 1984;23:5036-5041.
30. Chrzanowska-Wodnicka M, Burridge K. Rho-stimulated contractility drives the formation of stress fibers and focal adhesions. *J Cell Biol.* 1996;133:1403-1415.
31. Uehata M, Ishizaki T, Satoh H, et al. Calcium sensitization of smooth muscle mediated by a rho-associated protein kinase in hypertension. *Nature.* 1997;389: 990-994.
32. Kumar J, Rao PV, Rowlette LL, Borras T, Epstein DL. Rho GTPase-mediated actin cytoskeletal reorganization in outflow pathway cells may modulate outflow function [abstract]. *Invest Ophthalmol Vis Sci.* 1999;40:S669.
33. Lütjen-Drecoll E. Structural factors influencing outflow facility and its changeability under drugs: a study in *Macaca arctoides*. *Invest Ophthalmol.* 1973;12: 280-294.
34. Kaufman PL, Bárány EH. Loss of acute pilocarpine effect on outflow facility following surgical disinsertion and retrodisplacement of the ciliary muscle from the scleral spur in the cynomolgus monkey. *Invest Ophthalmol.* 1976;15: 793-807.
35. Johnson M, Shapiro A, Ethier CR, Kamm RD. Modulation of outflow resistance by the pores of the inner wall endothelium. *Invest Ophthalmol Vis Sci.* 1992;33: 1670-1675.
36. Grierson I, Lee WR. Acid mucopolysaccharides in the outflow apparatus. *Exp Eye Res.* 1975;21:417-431.
37. Segawa K. Electron microscopic changes of the trabecular tissue in primary open-angle glaucoma. *Ann Ophthalmol.* 1979;11:49-54.
38. Rohen JW. Why is intraocular pressure elevated in chronic simple glaucoma? *Ophthalmology.* 1983;90:758-765.
39. Lütjen-Drecoll E, Shimizu T, Rohrbach M, Rohen JW. Quantitative analysis of "plaque material" in the inner- and outer wall of Schlemm's canal in normal- and glaucomatous eyes. *Exp Eye Res.* 1986;42:443-455.
40. Acott TS. Trabecular extracellular matrix regulation. In: Drance SM, Van Buskirk EM, Neufeld AH, eds. *Pharmacology of Glaucoma.* Baltimore, Md: Williams & Wilkins; 1992:125-157.
41. Hubbard WC, Johnson M, Gong H, et al. Intraocular pressure and outflow facility are unchanged following acute and chronic intracameral chondroitinase ABC and hyaluronidase in monkeys. *Exp Eye Res.* 1997;65:177-190.
42. Acott TS, Westcott M, Passo MS, Van Buskirk EM. Trabecular meshwork glycosaminoglycans in human and cynomolgus monkey eye. *Invest Ophthalmol Vis Sci.* 1985;26:1320-1329.
43. Acott TS. Biochemistry of aqueous humor outflow: glaucoma. In: Kaufman PL, Mittag T, eds. *Glaucoma.* London, England: Mosby–Year Book Europe Ltd; 1994: 1.47-1.78.
44. Knepper PA, Goossens W, Hvizd M, Palmberg PF. Glycosaminoglycans of the human trabecular meshwork in primary open-angle glaucoma. *Invest Ophthalmol Vis Sci.* 1996;37:1360-1367.
45. Knepper PA, Goossens W, Palmberg PF. Glycosaminoglycan stratification of the juxtacanalicular tissue in normal and primary open-angle glaucoma. *Invest Ophthalmol Vis Sci.* 1996;37:2414-2425.
46. Lütjen-Drecoll E, Bárány EH. Functional and electron microscopic changes in the trabecular meshwork remaining after trabeculectomy in cynomolgus monkeys. *Invest Ophthalmol.* 1974;13:511-524.
47. Erickson-Lamy KA, Kaufman PL, McDermott ML, France NK. Comparative anesthetic effects of aqueous humor dynamics in the cynomolgus monkeys. *Arch Ophthalmol.* 1984;102:1815-1820.
48. Keller HU, Niggli V, Zimmermann A, Portmann R. The protein kinase C inhibitor H-7 activates human neutrophils: effect on shape, actin polymerization, fluid pinocytosis and locomotion. *J Cell Sci.* 1990;96(pt 1):99-106.